Vol. 43: 23–32, 2006 | AQUATIC MICROBIAL ECOLOGY
Aquat Microb Ecol | Published May 3

Bacterioplankton of low and high DNA content in the suboxic waters of the Arabian Sea and the Gulf of Oman: abundance and amino acid uptake

Mikhail V. Zubkov[1,*], Glen A. Tarran[2], Peter H. Burkill[1]

[1]National Oceanography Centre, European Way, Southampton SO14 3ZH, UK
[2]Plymouth Marine Laboratory, Prospect Place, West Hoe, Plymouth PL1 3DH, UK

ABSTRACT: Amino acid uptakes by bacterioplankton of low DNA (LNA) and high DNA (HNA) content, populating the oxygen minimum zone (OMZ: <5 µM O_2) and adjacent oxygen-depleted waters (5 to 50 µM O_2), were determined using a ^{35}S-methionine precursor and flow cytometric sorting. The HNA cells were further differentiated into low light scatter (HNA-ls) and high cell light scatter (HNA-hs) groups. Total bacterioplankton methionine uptake strongly correlated ($r > 0.998$, $p < 0.0001$) with leucine incorporation into protein and with microbial glucose uptake, suggesting that bacterioplankton growth was controlled by dissolved organic matter, and that methionine uptake could be used as a general estimate for the metabolic activity of bacterioplankton. The variation in methionine uptake depended on the prokaryote group rather than on ambient oxygen concentration, e.g. the numerically dominant LNA cells took 3 to 5 times less precursor than the HNA cells. A percentage of the LNA cells with double the amount of DNA was proposed as an incubation-independent index of growth of the cells in the G_2 stage of the cell cycle. The vertical profiles of the percentage of LNA cells in G_2 showed pronounced peaks at 300 to 600 m in the OMZ that did not correlate with peaks of either total bacterioplankton abundance or productivity. The present paper underlines the importance of bacterioplankton group studies in the OMZ since high microbial cell abundance does not necessarily mean high metabolic activity and other mechanisms, such as resilience to mortality pressure, have to be investigated.

KEY WORDS: Bacterioplankton · Flow cytometric sorting · Oxygen minimum zone · Isotopic tracer · Metabolic activity

INTRODUCTION

The Arabian Sea (ArS) and Gulf of Oman (GoO) generate a wide range of biogeochemical conditions due to the interaction of seasonal monsoons and an enclosed ocean basin. The seasonally high production is exported into the waters of the ocean's interior where it has a long residence time. This creates a pronounced mid-water oxygen minimum zone (OMZ) that is interleaved with subsurface outflow of high salinity and low oxygen containing waters from the Red Sea. This water has been suggested as the basis for the origin of the unique vertical stratification in the ArS (Tomczak & Godfrey 1994). Oxygen depletion is made greater by excessive microbial oxygen respiration, leading to intensive microbial denitrification in the middle part of the ArS (Naqvi 1994, Jayakumar et al. 2004). In the GoO, subsurface warm saline water with low oxygen flows in from the Persian Gulf, forming a layer of low oxygen water in the GoO (Tomczak & Godfrey 1994). This layer extends into the northwestern ArS. Where this happens, 2 suboxic layers are present with the top of the shallower suboxic layer at less than 30 m from the surface, and total bacterioplankton abundance increases to almost surface mixed layer concentrations at the top of the OMZ (Ducklow 1993).

The OMZ is a site of extensive denitrification (Naqvi 1994) and a link between functional diversity of nitrite reductase genes and inorganic nitrogen chemistry was recently found (Jayakumar et al. 2004). Despite a few studies of the composition of the prokaryotic communities in the ArS (Riemann et al.

*Email: mvz@noc.soton.ac.uk

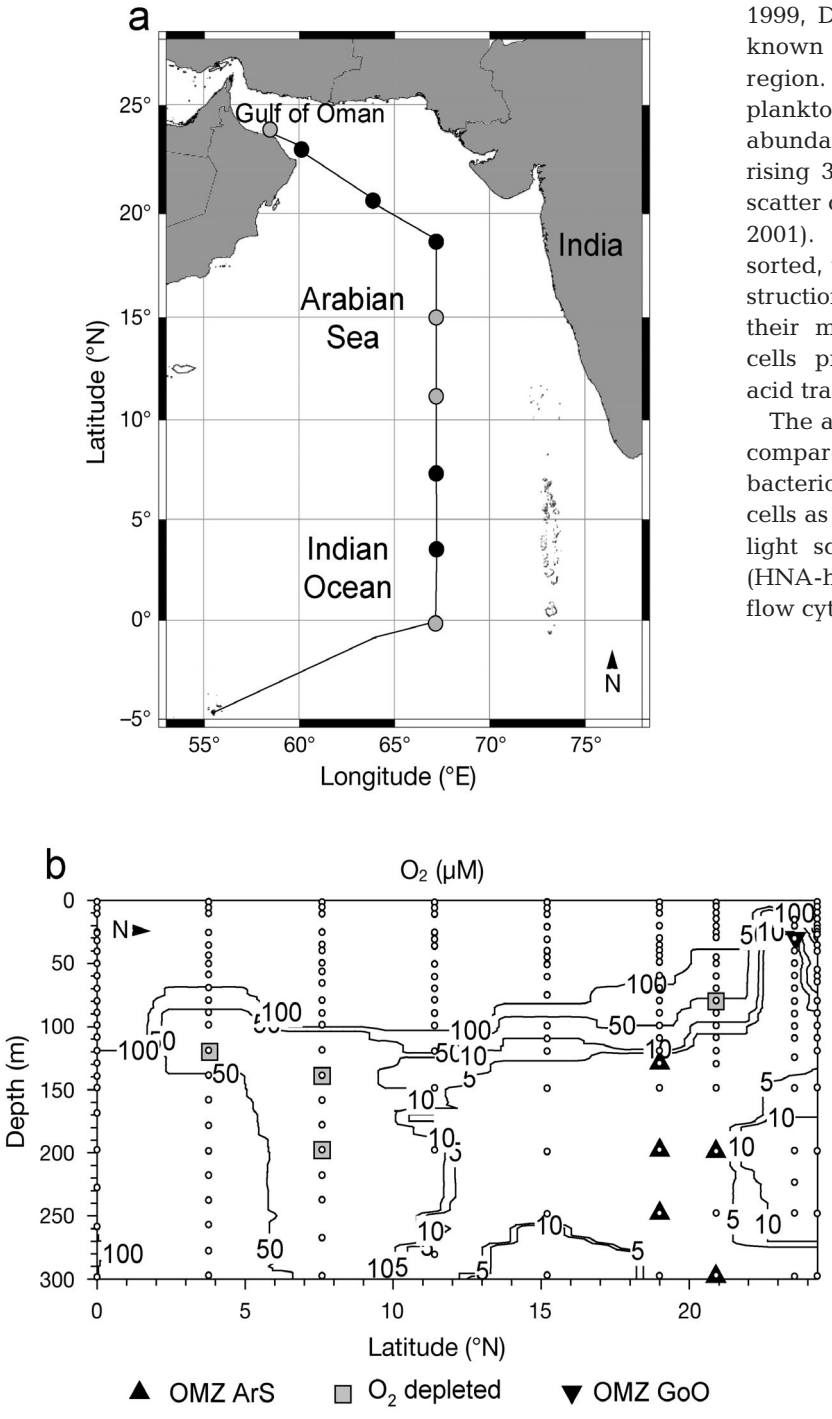

Fig. 1. Environmental conditions in the sampled waters. (a) Cruise track and station locations (circles). Black circles: stations at which flow cytometric sorting of bacterioplankton was carried out, amino acid uptake rates estimated and bacterioplankton concentrations determined. Grey circles: stations at which total community precursor uptake rates and bacterioplankton concentrations were determined. (b) Contour plot of vertical distribution of oxygen (µM) along the transect. Large symbols indicate the depths at which samples for flow sorting were collected in the oxygen minimum zone (OMZ) of the Arabian Sea (ArS) and of the Gulf of Oman (GoO) as well as in the adjacent oxygen-depleted waters. Depths sampled for bacterioplankton abundance are indicated by small open circles

1999, Damste et al. 2002, Fuchs et al. 2005) little is known about their structure in the OMZ in this region. As an initial step towards studying bacterioplankton structure, it is possible to look at the most abundant groups using flow cytometry by categorising 3 or more groups based on DNA versus light scatter characteristics (Gasol et al. 1999, Lebaron et al. 2001). These groups can be flow cytometrically sorted, the cells used for 16S rRNA clone library construction (Wallner et al. 1997, Fuchs et al. 2005) and their metabolic activities can be determined from cells preloaded with radioactively labelled amino acid tracer (Zubkov et al. 2001).

The aim of the present study was to measure and to compare metabolic activities of numerically dominant bacterioplankton groups of low DNA (LNA) containing cells as well as of high DNA containing cells with low light scattering (HNA-ls) and high light scattering (HNA-hs) in the OMZ of the ArS and GoO using the flow cytometric sorting technique.

MATERIALS AND METHODS

Study area and sample collection. The work was carried out on cruise CD132 of the RRS 'Charles Darwin' in the ArS and the GoO in September 2001. The cruise was planned as a transect of 9 stations from the equator to 24°19′ N, initially along the 67° E meridian and later turning northwest into the GoO (Fig. 1a). Seawater was collected with a rosette of 24 × 20 l Ocean Test Equipment water samplers mounted on a Sea-Bird 9/11 plus conductivity-temperature-density (CTD) system with a Sea-Bird 43B Oxygen sensor s/n 43B-0013 calibrated by the manufacturer. Oxygen-depleted waters (5 to 50 µM O_2) were observed from the equator to 24° N (Fig. 1b). The OMZ (<5 µM O_2) was detected between 11 and 24° N at depths below 100 m (Fig. 1b). At each station, up to 24 depths were sampled to determine bacterioplankton abundance in the top 300 m at each of 2 to 3 CTD casts at about 12 h intervals. Ten selected samples were collected for flow sorting of bacterioplankton groups to determine group-specific methionine (Met) uptake rates (Fig. 1b, symbols) as well as for bulk bacterioplankton uptake rates of leucine (Leu) and glucose (Glu). From 11° N, deeper casts were also sampled to determine bacterioplankton abundance down to 2000 m. Additionally, bulk bacterioplankton uptake rates of Met and Leu were measured down to 600 m at 21° N.

Determination of bacterioplankton abundance. Water samples of 1.8 ml were fixed with paraformaldehyde (20% PFA freshly dissolved in particle free seawater, 1% final concentration) and incubated at 2° C for 24 h. The samples were then stained with SYBR Green I DNA dye (Marie et al. 1997) and analysed with a FACSort flow cytometer (Becton Dickinson) on board the ship. Yellow-green beads of 0.5 µm diameter (Fluoresbrite Microparticles, Polysciences) were used in all analyses as an internal standard (Fig. 2a). Total bacterioplankton abundance was determined at all depths sampled. Three main bacterioplankton groups were selected, based on their DNA content and light scatter properties (Fig. 2b). One population contained cells with low nucleic acid content (low SYBR Green I fluorescence) and low side scatter, the LNA. A second population contained cells with high nucleic acid content and low side scatter, the HNA-ls and a third population contained cells with high nucleic acid content and high light scatter, the HNA-hs. A clear subcluster of the LNA cells with approximately 2 times higher average green fluorescence, corresponding to double the amount of DNA per cell, and nearly twice as high light scatter compared to the main cluster was observed in the OMZ samples. The subcluster was interpreted as the LNA cells that could be at the G_2 stage of their cell cycle, completing synthesis of the second copy of DNA. The determination of DNA content of cells at different stages of cell cycle for assessing cell population growth is a common and widely used procedure in flow cytometry (e.g. Marie et al. 1997, Shapiro 2003).

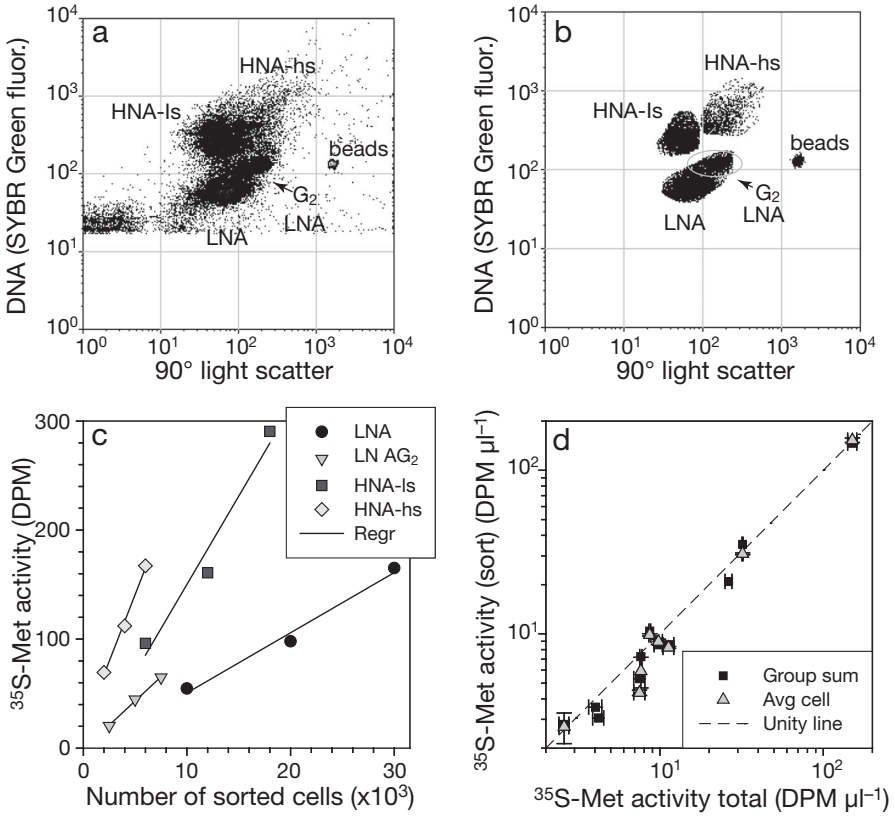

Fig. 2. Flow cytometric sorting of bacterioplankton for the methionine (Met) activity determination: (a) Signature of stained bacterioplankton which populated the oxygen minimum zone. The sample was collected from 298 m at 20° 55′ N 63° 40′ E. (b) The flow sorted cytometric groups of cells identified with high nucleic acid content and high or low 90° light scatter, HNA-hs or HNA-ls, respectively, and LNA cells with low nucleic acid content. LNA group also contains a subgroup with approximately twice the SYBR Green I – DNA fluorescence (arrow), i.e. an index of doubled genome of cells at G_2 stage of cell cycle. (c) An example of the flow sorting radioassay of bacterioplankton groups identified in (b). Lines show linear regressions (Regr). (d) Correlation between the Met activity of the whole bacterioplankton community (total), a sum of flow sorted groups (Group sum) and flow sorted average bacterioplankton cell (Avg cell) multiplied by bacterioplankton concentration to assess the accuracy of sorter alignment (details in text). Error bars show 1 SE

Determination of total microbial productivity. The samples used for uptake rate determinations were collected into acid-washed 1 l thermos flasks using acid soaked silicone tubing and processed within 1 h of sampling. Incubation vessels were gently filled with samples to avoid agitation and reaeration, although strictly, anaerobic sample handling was not possible because of the significant technological complexity required for *in situ* incubations. Two amino acids (^{14}C-Leu and ^{35}S-Met; Leu and Met) and a sugar (^{14}C-Glu; Glu) were used as precursors (Amersham Biosciences). Samples were incubated in the dark at the *in situ* temperatures but at atmospheric pressure.

Samples (1.6 ml) were pipetted into sterile polypropylene microcentrifuge tubes and inoculated with L-[^{35}S]methionine (>1000 Ci mmol^{-1}), ~1 nM final concentration. The subsamples (0.5 ml) were fixed with 1% PFA (final concentration) at 1.5, 3 and 4.5 h. Samples (33 ml) were pipetted into acid washed Teflon bottles and inoculated with L-[U-^{14}C]leucine, (295 mCi mmol^{-1}), 20 nM final concentration, or D-[U-^{14}C]glucose (310 mCi mmol^{-1}), 20 nM final concentration, to determine rates of uptake at above ambient, precursor concentrations, saturating bacterioplankton uptake (Chin-Leo & Kirchman 1988, Skoog et al. 1999, M. Zubkov unpubl. data). The subsamples (10 ml) were fixed in 50 ml polypropylene centrifuge tubes at 1.5, 3 and 4.5 h

(0.5, 1 and 1.5 h at 3° 48′ N and 23° 32′ N stations), either by mixing with an equal volume of 10% (w/v) trichloroacetic acid (TCA) for Leu incorporation, or by adding 20% PFA dissolved in 0.2 µm filtered seawater, to 1% final concentration for Glu uptake. The particulate material in the samples was harvested onto 0.2 µm nylon filters (Supor, Pall) pre-soaked in 1 mM of Leu or Glu, respectively. The filters were rinsed twice with 5 ml of deionised water. Radioactivity retained on filters was measured as disintegrations min^{-1} (DPM) with a Rack-Beta 1409 liquid scintillation counter (LKB-Wallac). The rate of precursor incorporation was calculated as the slope of the linear regression of radioactivity against incubation time ($r^2 > 0.96$, $p < 0.1$, $n = 3$). Uptake or incorporation rate constants, i.e. fractions of the added precursor consumed by bacterioplankton h^{-1}, were multiplied by the added precursor concentrations and used for rate comparison.

Determination of methionine uptake by bacterioplankton groups. Metabolic activities of bacterioplankton groups were determined from a total of 10 samples using the incorporation rate of ^{35}S-Met (Zubkov et al. 2001). Met was added at ~1 nM concentration. Five replicated 1.6 ml samples from 1 to 3 depths in oxygen-depleted or within the OMZ were incubated at *in situ* temperatures in the dark and fixed with PFA (1% final concentration) after 6 h (3 h, at the 3° 48′ N and 23° 32′ N stations) incubation and kept frozen at –20° C. Such a long incubation was necessary to load bacterioplankton cells with a sufficient amount of labelled precursor for sorting ashore 2 to 3 mo after the cruise. A comparison of absolute bacterioplankton counts done on board the ship before samples were frozen and counts made at the time of cells sorting using regression analysis (slope = 0.90 ± 0.02, $r^2 = 0.98$, $n = 9$, $p < 0.0001$) showed close agreement with 10% cell loss, and a corresponding correction was applied in calculations.

Thawed samples were stained with SYBR Green I (Marie et al. 1997) and bacterioplankton groups were selected, based on their DNA content and light scatter properties (Fig. 2b). Scatter signal intensities depend on refractive index as well as on cell size and is a useful parameter to discriminate different cell types (Shapiro 2003). In 8 out of 10 samples all bacterioplankton cells were gated and sorted to determine the activity of an average bacterioplankton cell as an additional check of sorting accuracy. All groups were flow sorted using FACSort and FACSCalibur flow cytometers (Becton Dickinson) with standard configuration. Both instruments were set to single-cell sort mode, sorting between 10 and 150 particles s^{-1}. Sorted cells were collected onto 0.2 µm pore size nylon filters, rinsed with deionised water and radio-assayed. Three proportional numbers of cells (from 1, 2 and 3×10^3 to 10, 20 and 30×10^3 cells) were sorted, and the cell Met uptake was determined as the slope of the linear regression of radioactivity against the number of sorted cells ($r^2 > 0.96$, $p < 0.1$, $n = 3$; e.g. Fig. 2c).

Population specific activity of flow sorted bacterial groups was determined by multiplying the radioactivity of the average group cell sorted by the abundance of the group. The relative population activity was calculated as the population fraction of total bacterioplankton community. To directly determine the Met uptake of the whole microbial community, the 100, 200 and 300 µl aliquots of remaining unsorted samples were filtered and filters were subsequently radio-assayed.

The accuracy of gate sorting was determined by comparing the activities of the whole bacterioplankton communities, a sum of the bacterial group populations, which comprised the communities and a mean sorted bacterioplankton cell multiplied by bacterioplankton abundance (Table 1). All paired correlations between the 3 measurements were very strong indeed (Pearson correlation coefficient $r > 0.999$, $p < 0.0001$; Fig. 2d), confirming the high accuracy of sorting.

RESULTS AND DISCUSSION

Comparison of bacterioplankton uptake of methionine, leucine and glucose

The incubation time for flow sorting of 6 h was chosen for practical reasons, i.e. to maximise the amount of radiolabel taken up by bacterioplankton cells as flow sorting could only be carried out 2 mo after the cruise

Table 1. Methionine uptake (units: DPM $µl^{-1}$) by the whole bacterioplankton community (Total), a sum of flow sorted groups (Group sum) and of cell-sorted average bacterioplankton multiplied by total bacterioplankton abundance (Avg. cell). NS = not sorted

Latitude (°N)	Depth (m)	Oxygen (µM)	Total (mean ± SE)	Group sum	Avg. cell (mean ± SE)
3.8	120	38.7	2.59 ± 0.18	2.79	2.7 ± 0.58
7.6	140	38.6	4.03 ± 0.37	3.56	NS
7.6	200	13.1	4.20 ± 0.33	3.05	NS
19.0	130	3.7	11.29 ± 0.86	8.58	8.24 ± 0.11
19.0	200	2.5	7.64 ± 0.11	7.24	5.92 ± 1.26
19.0	250	2.6	8.66 ± 0.11	10.38	9.85 ± 0.16
20.9	80	44.7	32.06 ± 0.28	35.2	30.85 ± 0.38
20.9	200	3.5	7.49 ± 0.59	5.32	4.36 ± 0.16
20.9	300	2.7	9.79 ± 0.58	8.58	8.95 ± 0.33
23.6	30	2.4	151.0 ± 9.65	146.4	152.7 ± 4.76

and ^{35}S isotope has a relatively short half-life of 87.5 d. The measured end-point Met uptake of the whole community showed strong correlation with Met uptake rate in the OMZ and the oxygen-depleted waters (Fig. 3a), indicating that the 6 or 3 h end-point Met uptake was proportional to the Met uptake rate estimated in time series.

To test the suitability of Met uptake for quantifying bacterioplankton cell protein synthesis, the microbial uptake rates of ^{35}S-Met (~1 nM) against rates of ^{14}C-Leu (20 nM) incorporation into TCA insoluble material, i.e. proteins, and uptake rates of ^{14}C-Glu (20 nM) were compared. The 3 uptake rate measurements strongly correlated (Fig. 3b,c), confirming the adequacy of the Met uptake measurement for the estimation of bacterioplankton productivity.

The rate measurements reported above were all made in samples collected from depths down to 300 m, where ambient oxygen concentration was 2 to 40 µmol l^{-1} compared to >150 µmol l^{-1} in oxygen-replete surface waters. Taking into account that all sampled waters were suboxic rather than anoxic, one should not expect instantaneous poisoning of microorganisms due to oxygen concentration increases as a result of sampling and incubation on board ship. To carry out uncompromised sampling and incubations of such waters, special pressure-retaining vessels, preserving low oxygen concentrations would be required. In the absence of such sophisticated equipment, samples were only maintained at *in situ* temperature and gas exchange was reduced by conducting experiments in gas tight, e.g. teflon, bottles with minimal head space. The effect of decompression on microorganisms raised from 300 to 600 m depths was probably minimal (Carlucci et al. 1986, Turley 1993). Considering the relative shortness of incubation periods (≤6 h) any changes in oxygen concentrations appeared to have a limited effect on the uptake rates (Ducklow 1993), and indeed the time series in the present study showed linear uptake of precursors (Table 2), supporting this suggestion.

The estimated number of Met molecules taken up by an individual cell h^{-1} varied from 200 to 60 000, depending more on the group concerned than on oxygen concentration (Fig. 4). Specific cell Met uptake was lower in LNA cells compared to HNA cells. The highest Met uptake was found in cells from the top of the OMZ in the GoO (Figs. 1b & 4). However, the cell uptake rates of the 3 groups in the OMZ of the ArS were generally lower than in the oxygen-depleted (5 to 50 µM) waters. The LNA G_2 cells were metabolically more active, taking about 1.4 times more Met molecules than the average LNA cells in the same sample. The lowest values of cell activity were found in the OMZ in the ArS (Fig. 4). Intermediate values, 1.7 to

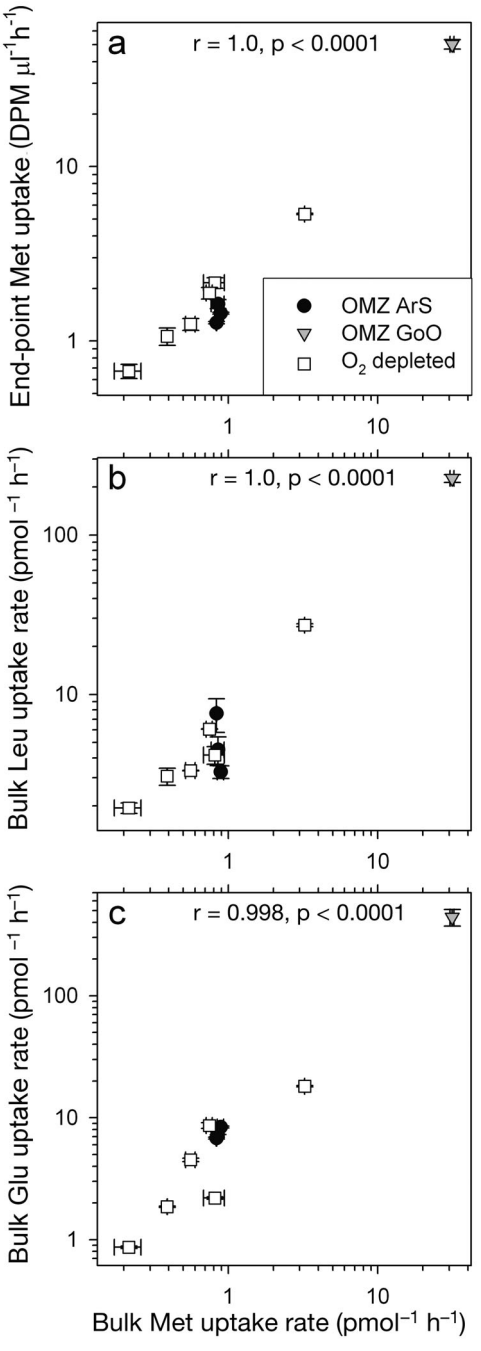

Fig. 3. Comparison of uptake of different substrates by bacterioplankton in different regions, the OMZ of the Arabian Sea (ArS) and the Gulf of Oman (GoO) and adjacent oxygen-depleted waters (O_2 depleted). (a) Relationship between the methionine (Met) uptake rate by total bacterioplankton in bulk samples and the end-point Met uptake by the sum of bacterioplankton groups labelled for flow sorting. (b) Relationship between the Met uptake rate and Leu incorporation rate by total bacterioplankton. (c) Relationship between the Met uptake rate and Glu uptake rate by total bacterioplankton. Note the log scales used on all axes. Corresponding Pearson correlation coefficient values (r) and probability values (p) are given in each plot. Error bars show 1 SE

Table 2. Methionine (Met), leucine (Leu) and glucose (Glu) uptake (units, pmol l^{-1} h^{-1}) by the bulk bacterioplankton in the OMZ and O_2 depleted waters of the ArS and the GoO. The rates were calculated as slopes of linear regressions of time series, $p < 0.1$, $n = 3$

Latitude (°N)	Oxygen (µM)	Met		Leu		Glu	
		Slope ± SE	r^2	Slope ± SE	r^2	Slope ± SE	r^2
3.8	38.7	0.81 ± 0.13	0.975	4.17 ± 0.53	0.984	2.19 ± 0.05	0.999
7.6	38.6	0.39 ± 0.01	0.985	3.08 ± 0.38	0.985	1.86 ± 0.02	0.999
7.6	13.1	0.22 ± 0.04	0.999	1.94 ± 0.15	0.994	0.87 ± 0.02	0.999
19.0	3.7	0.75 ± 0.03	0.998	6.06 ± 0.03	0.999	8.82 ± 0.48	0.997
19.0	2.5	0.83 ± 0.01	0.996	7.59 ± 1.81	0.946	6.80 ± 0.11	0.999
19.0	2.6	0.89 ± 0.04	0.999	3.27 ± 0.30	0.992	8.39 ± 0.14	0.999
20.9	44.7	3.24 ± 0.01	0.999	27.2 ± 0.52	0.999	18.1 ± 0.25	0.999
20.9	3.5	0.56 ± 0.04	0.956	3.33 ± 0.01	0.999	4.51 ± 0.14	0.999
20.9	2.7	0.85 ± 0.09	0.975	4.50 ± 0.92	0.960	7.96 ± 0.69	0.993
23.6	2.4	31.4 ± 0.97	0.996	226.3 ± 13.0	0.997	440.8 ± 68.1	0.977

2 times higher than in the OMZ of the ArS were found in the oxygen-depleted waters where oxygen content was between 5 to 50 µM (Fig. 4). The highest recorded values were found in the OMZ of the GoO, where cell activity values were 15 to 21 times higher than in the OMZ of the ArS. The remarkable proportionality between the 3 flow cytometrically defined groups was another confident indicator that cell Met uptake corresponded to the general metabolism of cells in the OMZ. Similar proportionality was observed in the surface waters of the ArS (M. Zubkov unpubl. data) and in coastal seas (Zubkov et al. 2001). Therefore, low cell uptake rates of the LNA group indicated that the LNA group was a minor contributor to Met uptake and consequently to bacterioplankton metabolism and production in the OMZ.

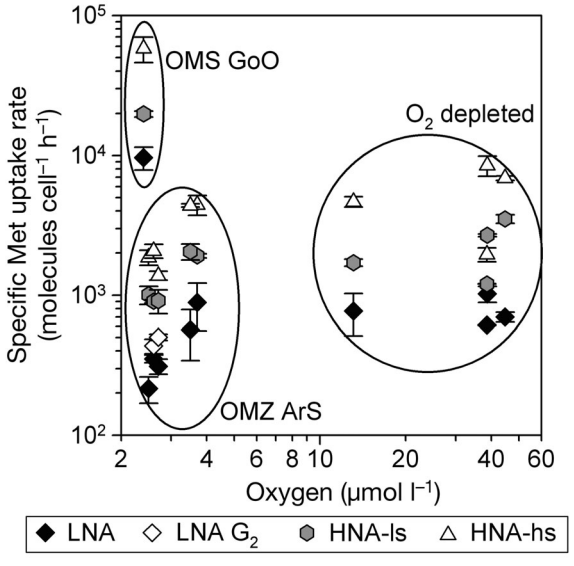

Fig. 4. Relationship between oxygen concentration and cell-specific Methionine (Met) uptake rates of the flow sorted bacterioplankton groups. Error bars show 1 SE. Different regions: the OMZ of the Arabian Sea (ArS), and the Gulf of Oman (GoO). Adjacent oxygen-depleted waters (O_2 depleted) are encircled by solid lines. Note the log scale axes

Comparison of vertical distribution of oxygen and bacterioplankton in the OMZ

Because of the complexity and duration of analyses involved, the Met uptake rate measurements in conjunction with flow sorting of bacterioplankton groups could only be done at selected key points in the oxygen concentration field (Figs. 1 & 5a–e). Waters moderately depleted of oxygen (~40 µM) were observed as far as the 03° 48′ N station but low oxygen seemed to have no effect on bacterioplankton abundance or community structure, as defined by flow cytometry (Fig. 6). Bacterial abundance decreased gradually with increased water density, i.e. depth (Fig. 5a), supporting earlier observations (Ducklow 1993). A similar situation was observed at the 07° 36′ N station with ~15 µM oxygen concentration (Fig. 5b). The OMZ waters with an order of magnitude lower oxygen concentrations in their core, at 19 to 23.5° N were populated by abundant bacterioplankton, which reached its highest abundance when the oxygen minimum was closest to the surface (Fig. 5c–e). Uptake rates varied from 0.2 pmol Met l^{-1} h^{-1} in oxygen-depleted waters at the 07° 36′ N station to 30 pmol Met l^{-1} h^{-1} at the top of the OMZ in the GoO. The rates in the core of the OMZ in the ArS at 19 to 23.5° N were constantly low at about 0.9 pmol Met l^{-1} h^{-1}.

The HNA-ls group of bacteria contributed the most (30 to 60%) to Met uptake, followed by and on some occasions exceeded by the HNA-hs group (20 to 45%). The LNA group contributed only 10 to 25% (Fig. 6a). The relative group uptake rates did not cluster depending on the region studied and varied just as much

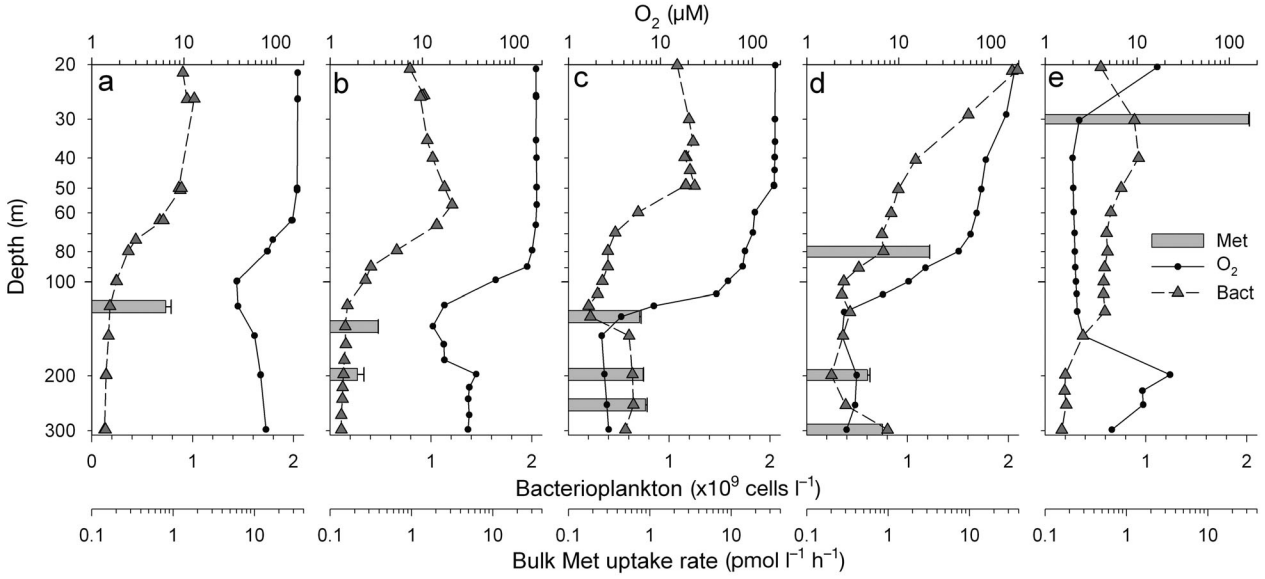

Fig. 5. Vertical profiles of oxygen, bacterioplankton concentration and methionine (Met) uptake rates at stations selected for bacterioplankton group flow sorting from the OMZ and adjacent oxygen-depleted waters in the ArS and the GoO: (a) Stn 3° 48′ N, (b) Stn 7° 36′ N, (c) Stn 19° N, (d) Stn 20° 55′ N, (e) Stn 23° 32′ N. Note the log scale axes

within the region as between the regions. The elevated bacterioplankton numbers observed in oxygen-depleted waters might indicate corresponding changes in bacterioplankton community composition. In this study, the relative numerical contribution of the 3 groups to the whole community was used as an index of compositional change (Fig. 6b). Although the rates varied by 2 orders of magnitude and bacterioplankton abundance by nearly one order of magnitude, the relative size of the 3 flow cytometric groups remained unchanged in the OMZ of the ArS. The LNA constituted about half (48 ± 6%) of the community, the HNA-ls group: 38 ± 6% of numbers; and the HNA-hs group: 14 ± 2% of numbers.

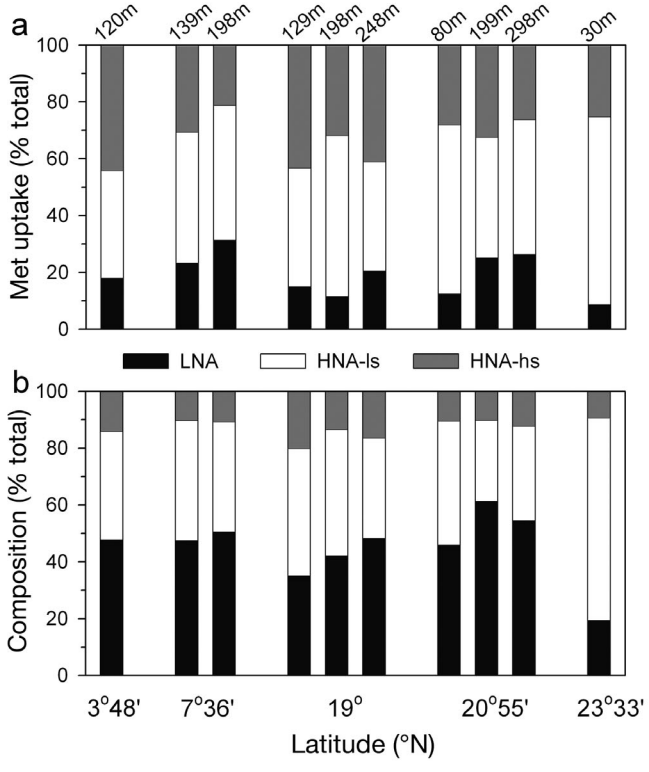

Fig. 6. Plots showing (a) relative importance of different bacterioplankton groups to methionine (Met) uptake and (b) bacterial community composition as defined by flow cytometry in flow sorted samples. Error bars show 1 SE

An exceptionally different community dominated by the HNA-ls (70% of the total numbers) was observed at the top of the OMZ in the GoO. The outflows of Red Sea and Persian Gulf waters along the transect towards the GoO (revealed on the temperature versus salinity diagrams (data not shown) with converging physical structure of the water column in deep waters was a characteristic of the ArS (Tomczak & Godfrey 1994). The anomaly was particularly pronounced at the 23° 32′ N station (Fig. 1). Increased water density closer to the surface reduced the vertical water density gradient and consequently, organic matter produced by an extensive phytoplankton bloom, e.g. 0.6×10^9 *Synechococcus* cells l^{-1} as well as 8.0×10^9 cells l^{-1} of other bacterioplankton (authors′ unpubl. data), in the top 10 m of the surface layer could mix faster into the sea interior providing nutrients to microorganisms living there. The resultant microbial respiration could further deplete the midwaters of dissolved oxygen (e.g. Fig. 5), facilitate and maintain the shallow OMZ in the case of reduced vertical mixing.

The transect of additional deep CTD casts afforded a good opportunity to observe spatial changes in the OMZ chemical and microbiological vertical structure down to 2000 m. The OMZ midwaters (~3 µM O_2) were observed at the 11° 23′ N station, becoming more and more pronounced at higher latitudes (Fig. 7a–e). Bacterioplankton concentrations elevated to a broad midwater peak of about 0.7×10^9 cells l^{-1} (Fig. 7c) that transformed into 2 midwater peaks of bacterioplankton abundance, observed at the next station (20° 55′ N, Fig. 8a). The peaks matched the oxygen minima separated by waters with double the oxygen concentration. This oxygen-elevated intermediate layer widened at the 23° 32′ N station with the extremely shallow top oxygen minimum at 30 m, with highest bacterioplankton abundance (0.9×10^9 cells l^{-1}) and activity within the OMZ (Fig. 5). In the GoO the oxygen elevated intermediate layer further broadened to ~400 m wide and bacterioplankton showed no evident concentration rise in the OMZ at this point (Fig. 7e).

Because the 16S rRNA gene clone library was dominated by the SAR11 sequences (Fuchs et al. 2005), a percentage of the LNA group numbers in the community was suggested as a rough index that could indicate a compositional change in the deep water bacterioplankton (Fig. 7f–j). The LNA group constantly comprised 40 to 50 % of all bacterioplankton cells. The LNA percentage only decreased to about 20 to 30 % at the top edges of the OMZ at the 23° 32′ N station. The vertical distribution of the LNA G_2 subpopulation was found to generally anticorrelate with the O_2 concentration along the transect down to 2000 m (Fig. 7). The peaks of this incubation-independent index of the LNA growth coincide with the deep part of the OMZ as well as with the top part of the double oxygen minima structure (Fig. 7c–e,h–j). The LNA G_2 index showed pronounced peaks even when neither bacterioplankton numbers nor the LNA index indicated changes (e.g. Fig. 7d–e, i–j).

The pronounced double peaks of O_2 minima and corresponding high bacterioplankton abundance ob-

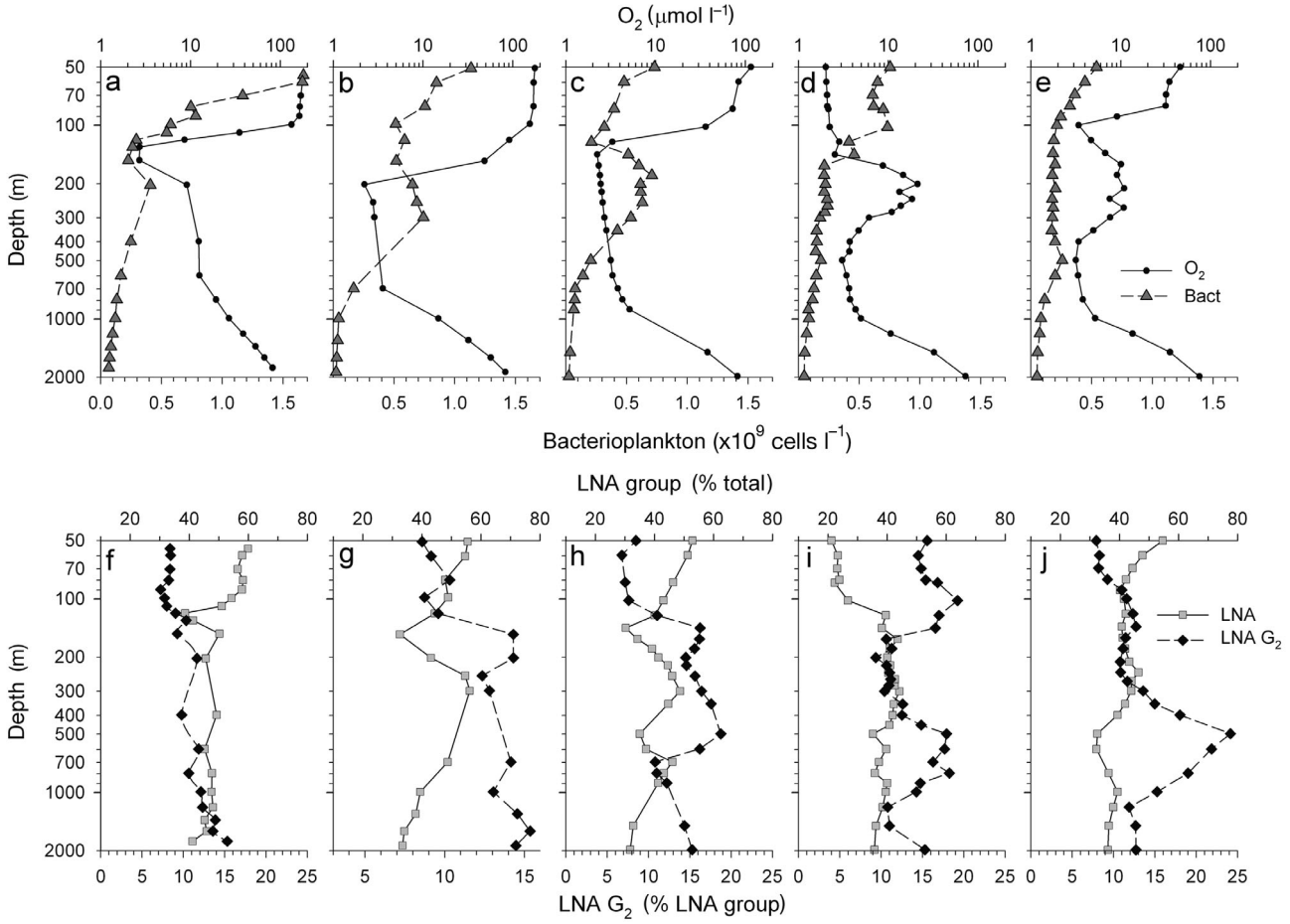

Fig. 7. Latitudinal series: (a) Stn 11° 23′ N, (b) Stn 15° 12′ N, (c) Stn 19° N, (d) Stn 23° 32′ N, (e) Stn 24° 19′ N, of deep (2000 m) vertical profiles of (a–e) oxygen and bacterioplankton concentration with corresponding profiles of (f–j) relative LNA and LNA G_2 (see Fig. 2 for details) bacterioplankton group abundance. Note the log scale axes

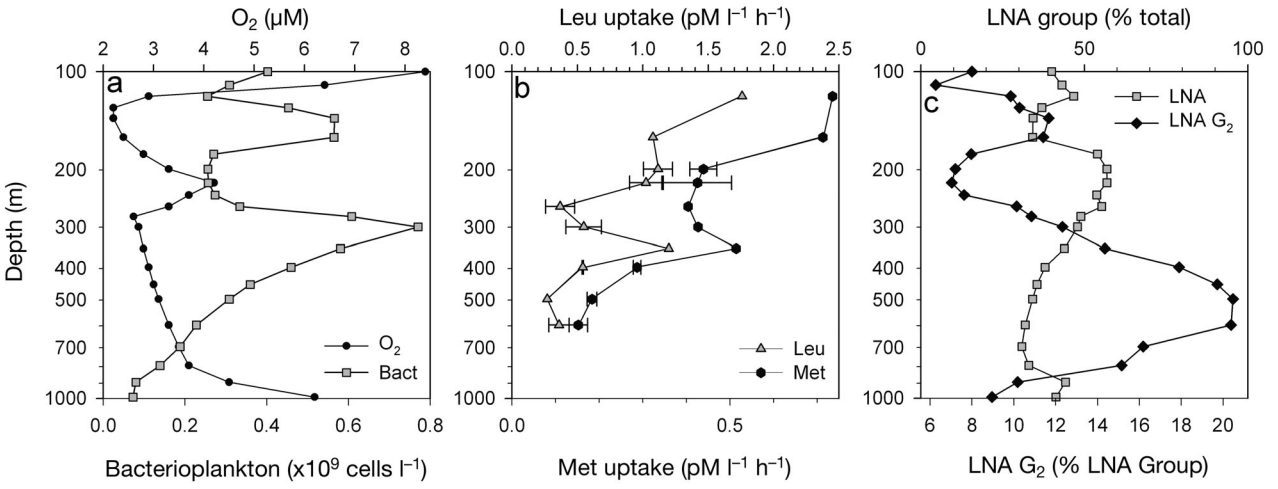

Fig. 8. Comparison of deep (1000 m) vertical distribution of (a) oxygen and bacterioplankton concentration, (b) leucine (Leu) and methionine (Met) uptake rates of bulk bacterioplankton and (c) LNA and LNA G_2 bacterioplankton group percentages at the 20° 55′ N station. Error bars show 1 SE. Note the log scale axes

served at 20° 55′ N (Fig. 8a) were studied in more detail by measuring rates of amino acid uptake rate, O_2 concentration and percentage of the LNA groups. Bacterioplankton abundance and O_2 vertical profiles corresponded to, but did not exactly match the peaks of bacterioplankton activity (Fig. 8b). Comparison of vertical profiles of Leu and Met uptake rates showed that the 2 bulk bacterioplankton productivity estimates were similar, with Met uptake rates generally being 50 to 60 % of Leu uptake rates. Despite high variability in bacterioplankton abundance and productivity the percentage of the LNA cells remained remarkably constant (Fig. 8c), indicating stability of bacterioplankton structure. However, the percentage of LNA G_2 cells showed a large, broad increase below the maximal bacterioplankton abundance and productivity, suggesting that the LNA group might grow relatively faster in the deep waters (400 to 500 m) below the peaks of total bacterioplankton abundance or productivity. Unfortunately, we were unable to flow sort the bacterioplankton populations, being limited at those depths by low cell abundance and activity. Even quantitative flow sorting of bacterioplankton populations at 300 m depth pushed the flow sorting technique to the very limit of its sensitivity. To our knowledge it was the first time the uptake rates of bacterioplankton groups were determined at those depths.

Microbial community structure in the OMZ

In many cases elevated bacterioplankton numbers were observed in oxygen-depleted waters and one might expect corresponding changes in the bacterioplankton composition. Bacterioplankton community structure assessed by flow cytometry revealed few differences between the OMZ compared to oxygen-depleted waters with one exception, the most productive waters of the Gulf OMZ (Figs. 5e & 6). Similarly, previous studies have shown that the number of dominant phylotypes was similar at different depths and only pronounced differences in composition, i.e. phylotype abundance, were seen with depth (Riemann et al. 1999). Considering that a depth-integrated sample could complicate interpretations of vertical variations in diversity (Riemann et al. 1999), a representative sample approach for molecular phylogenetic characterisation of the OMZ bacterioplankton was used (Fuchs et al. 2005). The approach was made even more specific by using flow sorting for separation of the LNA and HNA groups of bacterioplankton. The combined HNA group appeared to be phylogenetically diverse, as its heterogeneous flow cytometric signature indicated (Fig. 2a,b). The HNA clone library was dominated by members of the SAR406 cluster and bacteria related to symbiotic β-proteobacteria of *Bathymodiolus* (Fuchs et al. 2005). Both groups are uncultured and their role in the OMZ of the ArS remains speculative but it is quite likely that the redox-discontinuities indicate the presence of chemolithotrophic microorganisms in the waters investigated.

The tight flow cytometric signature of the LNA group suggested that it might be dominated by one or a few phylotypes (Fig. 2a,b). Indeed, the LNA clone library was dominated by the SAR11 sequences (Fuchs et al. 2005). However, despite extensive trials very few cells were identifiable using fluorescence *in situ* hybridisation, suggesting that the cells in the OMZ had very low metabolic activity. This is in agreement with the results of the present study.

CONCLUSIONS

Bacterioplankton groups in the OMZ regions of the ArS and GoO have been shown to take up Met for the first time. Rates of bacterial uptake varied greatly, from 200 to 60 000 molecules of Met $cell^{-1}$ h^{-1}, depending on the bacterial group concerned. Although the LNA group constantly represented about half of total bacterioplankton abundance in the OMZ of the ArS and in the oxygen-depleted waters, its Met uptake rate was always 3 to 5 times lower than the Met uptake by HNA cells. Consequently, the LNA group contributed only 10 to 20% to total bacterioplankton Met uptake. The flow cytometric signature of the LNA group suggested the presence of cells in the G_2 cell cycle stage, which were about 1.4 times more metabolically active than the mean LNA cells. The LNA cells seemed to replicate throughout the OMZ with the peak percentage of the LNA G_2 cells being found in waters generally below the peak of total bacterioplankton abundance and productivity. The LNA group's numerical dominance was not supported by a high Met uptake rate (i.e. metabolic activity), and further studies are required to explain the mechanism of the LNA abundance.

Acknowledgements. We acknowledge the captain, officers and crew aboard the RRS 'Charles Darwin' for their help during the cruise CD132. Thanks to Andrew Whiteley for enabling us to use the FACSCalibur instrument at CEH Oxford when our flow sorter was transported back from the cruise. We thank 3 anonymous reviewers for valuable comments on the manuscript. This work forms part of the Marine and Freshwater Microbial Biodiversity programme (NER/T/S/2000/00635) and was supported by the Natural Environment Research Council (NERC), UK, Plymouth Marine Laboratory and National Oceanographic Centre core science programmes and by the EU project BASICS grant EVK3-CT-00078. The research of M.V.Z. was supported by the NERC advanced research fellowship (NER/I/S/2000/00898).

LITERATURE CITED

Carlucci AF, Craven DB, Robertson KJ, Henrichs SM (1986) Microheterotrophic utilization of dissolved free amino-acids in depth profiles of southern-california borderland basin waters. Oceanol Acta 9:89–96

Chin-Leo G, Kirchman DL (1988) Estimating bacterial production in marine waters from the simultaneous incorporation of thymidine and leucine. Appl Environ Microbiol 54:1934–1939

Damste JSS, Rijpstra WIC, Hopmans EC, Prahl FG, Wakeham SG, Schouten S (2002) Distribution of membrane lipids of planktonic Crenarchaeota in the Arabian seat. Appl Environ Microbiol 68:2997–3002

Ducklow HW (1993) Bacterioplankton distributions and production in the Northwestern Indian-Ocean and Gulf-of-Oman, September 1986. Deep-Sea Res II 40:753–771

Fuchs BM, Woebken D, Zubkov MV, Tarran GA, Burkill PH, Amann R (2005) Molecular identification of picoplankton populations in contrasting waters of the Arabian Sea. Aquat Microb Ecol 39:145–157

Gasol JM, Zweifel UL, Peters F, Fuhrman JA, Hagstrom A (1999) Significance of size and nucleic acid content heterogeneity as measured by flow cytometry in natural planktonic bacteria. Appl Environ Microbiol 65: 4475–4483

Jayakumar DA, Francis CA, Naqvi SWA, Ward BB (2004) Diversity of nitrite reductase genes (nirS) in the denitrifying water column of the coastal Arabian Sea. Aquat Microb Ecol 34:69–78

Lebaron P, Servais P, Agogue H, Courties C, Joux F (2001) Does the high nucleic acid content of individual bacterial cells allow us to discriminate between active cells and inactive cells in aquatic systems? Appl Environ Microbiol 67:1775–1782

Marie D, Partensky F, Jacquet S, Vaulot D (1997) Enumeration and cell cycle analysis of natural populations of marine picoplankton by flow cytometry using the nucleic acid stain SYBR Green I. Appl Environ Microbiol 63: 186–193

Naqvi SWA (1994) Denitrification processes in the Arabian Sea. Proc Indian Acad Sci: Earth Planet Sci 103:279–300

Riemann L, Steward GF, Fandino LB, Campbell L, Landry MR, Azam F (1999) Bacterial community composition during two consecutive NE Monsoon periods in the Arabian Sea studied by denaturing gradient gel electrophoresis (DGGE) of rRNA genes. Deep-Sea Res II 46:1791–1811

Shapiro HM (2003) Practical flow cytometry. Wiley-Liss, Hoboken, NJ

Skoog A, Biddanda B, Benner R (1999) Bacterial utilization of dissolved glucose in the upper water column of the Gulf of Mexico. Limnol Oceanogr 44:1625–1633

Tomczak M, Godfrey JS (1994) Regional oceanography: an introduction. Pergamon, New York

Turley CM (1993) The effect of pressure on leucine and thymidine incorporation by free-living bacteria and by bacteria attached to sinking oceanic particles. Deep-Sea Res I 40:2193–2206

Wallner G, Fuchs B, Spring S, Beisker W, Amann R (1997) Flow sorting of microorganisms for molecular analysis. Appl Environ Microbiol 63:4223–4231

Zubkov MV, Fuchs BM, Burkill PH, Amann R (2001) Comparison of cellular and biomass specific activities of dominant bacterioplankton groups in stratified waters of the Celtic Sea. Appl Environ Microbiol 67:5210–5218

Editorial responsibility: Gerhard Herndl, Den Burg, Netherlands

Submitted: October 19, 2005; Accepted: January 30, 2006
Proofs received from author(s): April 21, 2006